WILEY | Hindawi

Research Article

Evaluating Congestion Management of Power System considering the Demand Response Program and Distributed Generation

Maede Zakaryaseraji and Ali Ghasemi-Marzbali [ID]

Department of Electrical and Biomedical Engineering, Mazandaran University of Science and Technology, Babol, Iran

Correspondence should be addressed to Ali Ghasemi-Marzbali; ali.ghasemi@ustmb.ac.ir

With increasing the energy demand, the optimal and safe operation of power systems is the main challenge for engineers. Thus, a technique for the optimal implementation of demand response programs (DRPs), installation of distributed generation (DG) with power transmission distribution factors, and DC dynamic load flow is presented in this paper. In fact, finding the optimal time execution of DRPs and the bus for installing wind units with its probabilistic effects is considered. In this model, the congestion is decreased and the available transfer capability (ATC) rates are significantly improved. According to various types of price-based DRPs, the customers motivate to change their utilization models by shifting the price of electricity at different times. Finally, the proposed model is evaluated on the well-known IEEE 39-bus New England power system. The numerical results show the efficiency of the proposed method because, after its application, the available transmissibility values in the critical buses have significantly increased. At the same time, system peak loads, total system costs, and losses are reduced, and the voltage profile also shows a significant improvement. Totally, numerical results demonstrate that using the recommended algorithm, system loss and cost decrease by 9 percent and $4472.

1. Introduction

The growth of electricity demand in current years brings some critical problems, e.g., transmission line congestion, lack of electricity production capacity, power outages, rising electricity prices, and atmosphere emissions based on fossil fuel power units. Continued growth in demand imposes additional costs for the construction of novel power units and transmission power lines. Consequently, it is essential to use several techniques of DRPs to decrease the utilization at peak times and improve the line congestion [1]. DRP is one of the successful techniques to help the customers make better smooth load profiles. In fact, clienteles make a significant role in congestion management (CM). However, this objective is obtained only if DRPs are applied optimally, with the intention that the best times (serious hours) to implement DRPs be supposed to be calculated by the independent system operator (ISO). It is worth noting that DRPs can be executed with several policies so that they are

usually employed to decrease the total load at peak times and accordingly decrease the electricity generation and its total costs. Also, if they are employed smartly, the total cost from both sides of customers and suppliers will be decreased, simultaneously [2]. Figure 1 presents the typical classification of DRPs.

Among many DR programs developed in restructured electricity markets and used in smart grids, DRPs are based on dynamic tariffs, e.g., TOU, RTP, and CPP where the benefits of these plans have been demonstrated in various articles and studies [3]. With the development of technology, the existence of such programs has been able to highlight the presence of distributed generation resources more than ever. One of the effects of installing distributed generation in power systems is reducing losses and improving voltage, reducing lines transmission power, and improving the system transmission capability [4]. In this regard, CM in transmission systems is known as the main challenge for designers of the ISO. It can be classified into two main
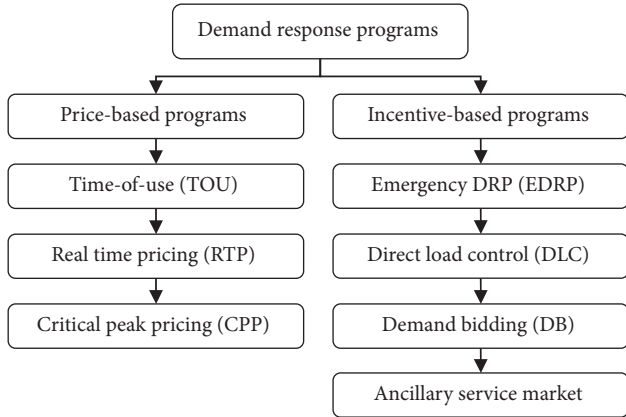
Figure 1: A typical categorization of DRPs.

groups: called corrective and preventive. The preventive group is defined based on transmission rights and ATC [5]. The second group is defined by informing users to revise their utilization model to improve the line congestion and accordingly enhance their profits [6]. Therefore, the best positions (critical tracks) and times (critical hours) for applying the DRPs must be calculated by ISO. On the other hand, determining the optimal location for the installation of wind generations in order to optimize the ATC is a challenge [7]. For this reason, the attitude of electricity market researchers and practitioners is to develop tools and techniques so that consumers can enjoy the benefits of being present in competitive markets, and at the same time, proper planning must be able to manage security constraints, reliability, and limitations of the transmission network [8]. Various studies have been conducted in the discussion of load management and smart grids. In [9], an effective pricing method is presented to create incentive schemes for the participation of more electricity consumers in electricity networks. Reference [10] presents a new model for decentralized management of the demand side. In this model, consumers are given the opportunity to be aware of the price of electricity at different hours of the day and night to be able to delay their consumption. In [11], a mechanism for managing the load consumption schedule is described as an integer linear programming problem. The main purpose of this article is to reduce the daily hourly load and somehow cause the load to balance; therefore, demand response programs are implemented according to different policies. These articles focus on reducing peak hourly load, and the effects of demand management programs on transmission line congestion have not been discussed.

On the other hand, the calculation of ATC with power transfer distribution factors (PTDFs) is given in [12–14]. PTDFs establish the sensitivity of several power system lines in different systems buses. Improving voltage and frequency maintenance of the islanded microgrid by managing the DR and distributed energy resources (DERs) are given in [15]. They are formulated based on the reactive and real power sensitivities in several buses to reduce the frequency and voltage fluctuations [15]. In [16], the automated residential DRPs considering the dynamic energy managing is offered.

Reference [17] defined DRP problems and possible solutions in smart grid and accomplished that DR is able to consider as a significant component of smart grids. In this type of research, the focus of the issue has been on finding DRP solutions in smart grids, while the study of the impact of these programs on transmission networks requires separate studies. In [18], a process for calculating the optimal incentives-based DRPs and, in [19], price-based methods for measuring the most favorable price during several times are proposed. In fact, the special effects of DR on cost diminution and utilization profile characteristics development are measured in these two papers. However, in [18,19], transmission line limitations and DR are not considered as an instrument for CM.

Considering the aforementioned advantages for the DRPs execution, the DRP is also employed to improve the power network's congestion. Other than that, it is achievable by determining the appropriate strategy, time, and price in DRPs. The article [6] proposed some methods based on incentive and redispatched generation units for the CM problem. A new design based on PTDFs is employed in [7] for the energy organization. There, distributed storage systems and DR supply assist the power trading between different microgrids. Although these articles have studied the effects of demand management programs on various objective functions of the system such as social welfare and ATC, the simultaneous effects of the use of DG and DRPs for the system's operating and planning have not been considered. In [20], a multiobjective particle swarm optimization (PSO) for CM problems using DRPs is presented. This reference shows that it is impossible to solve the network congestion problem without using the DRPs. In [8], an economical assessment of the flexible AC transmission system (FACTS) and the DR in modifying the ATC is offered. They showed that DLC improves ATC, but it has far above the ground costs. In [21], they presented a two-stage market-clearing method considering congestion management by FACTS and DR tools. In [20], a multiobjective PSO method for CM using DRPs is presented. This reference showed that it is impossible to solve the network congestion problem without using the DRP. Reference [22] provided a market-based mechanism that centrally controls the home energy management system. In this procedure, the distribution system operator (DSO) manages the congestion of electric vehicles charging using dynamic tariffs and daily electricity network tariffs. In [23], a stochastic method is suggested for CM in the electricity market. They emphasize the potential of using DR to improve the technical characteristics of the network, which has been considered in this article. In [24], a new method for optimal locations and times of DRPs is proposed. Optimal buses are identified based on the PTDFs, available transfer capability, and dynamic dc optimal power flow problem, while it is not considered the wind unit as a renewable resource. Reference [25] addressed this issue by developing a two-level integrated demand response (IDR) framework to reduce congestion in power networks. Reference [26] tried to present a secure procedure for wind-integrated transmission networks by suggesting a computationally efficient daily DC security-

constrained optimal power flow model. The article [27] focused on providing a cost-effective transmission switching approach to provide the minimum voltage safety margin index while dropping the active/reactive power capability of transmission lines. The article [28] recommends using the Shapley rate for this problem. It is an idea of cooperative game theory to share the entire surplus generated power by a coalition of players based on their marginal contributions. In [29], the dynamic tariff is first used as a price signal to address part of the density, and the scheduled reprofiling product is used as a product of incentive-based flexibility services to deal with residual density.

According to the aforementioned papers, the DRPs are employed to decrease the total costs and modify the requested energy profile or congestion constraints. However, there is not a completed model for DR employing in CM problem while satisfying the various objectives, e.g., the total cost reduction, PTDFs, and power system reliability improvements. It is noted that without selecting the best implementation and locations for DR and DG, the congested line may move to worse conditions. As a gap science in the previous papers, the optimal implementation of demand response programs with the selection of a suitable installation location of wind products that reduce power exchanges and improve portability is presented in this paper. In fact, in this paper, a process for the followed goals is suggested using ATC, PTDFs, and DDCOPF which is completely consistent with the real-world power system. In this paper, a combination of the mentioned pricing including the TOU and CPP is considered in this paper, and after employing ATC and DDCOPF computation, the best buses for implementing DRPs are determined. In addition, the simultaneous use of DG and DRPs is employed to identify and eliminate congested lines.

2. Problem Formulation

In this section, the noted problem formulation is developed. Primarily, the calculating method of PTDFs and ATC is presented. After that, the mathematical details of DDCOPF and the method of reducing the matrix of PTDFs are developed and the Optimal DC load flow is dynamically developed. Then, the DG model is introduced.

2.1. PTDFs and ATC Computation. As shown in Figure 2, PTDF indices are employed to present the amount of line flow sensitivities in power flow. PTDF is the ratio of power flow changes due to the power transaction from [24]. When the PTDF shows a high value, it means the power changes are able to effectively change the power flow and be suitable for DRPs:

Executing:

$$\text{PTDF}_{l,mn} = \frac{\Delta P_l}{\Delta P_{\text{bus}}} = \frac{X_{im} - X_{jm} - X_{in} + X_{jn}}{x_l}, \tag{1}$$

where X indicates reactance value and subscripts m, and i and j indicate the bus number. ΔP_l and ΔP_{bus} show the line and bus active power changes.
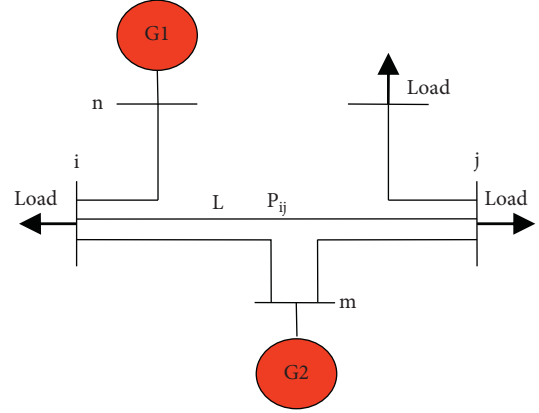

FIGURE 2: Display PTDF on the sample test system.

The transfer constraint for each power line (TL_l) considering the thermal overload is formulated as follows [12]:

$$\text{TL}_l = \begin{cases} \dfrac{P_l^{\max} - P_l}{\text{PTDF}_l}, & \text{PTDF}_l > 0, \\[2ex] \infty, & \text{PTDF}_l = 0, \\[2ex] \dfrac{P_l^{\max} - P_l}{\text{PTDF}_l}, & \text{PTDF}_l < 0, \end{cases} \tag{2}$$

where P_l and $P_l^{\max}$ indicate the power flow and the maximum possible value for power at the line l. Whatsoever the quantity of TL_l is less, the line l will be more constraining. Consequently, ATC is expressed by

$$\text{ATC} = \min\left(\text{TL}_l\right). \tag{3}$$

2.2. Dynamic DCOPF Procedure. Figure 3 shows the branch model, which contained a reactance associated in series with a perfect phase-shifting transformer by means of a complex transformer ratio $T = \tau \cdot e^{j\theta_{shift}}$. It can be calculated by

$$Y_{\text{branch}} = \frac{1}{jX_s} \begin{bmatrix} \dfrac{1}{\tau^2} & -\dfrac{1}{\tau \cdot e^{-j\theta_{\text{shift}}}} \\[3ex] -\dfrac{1}{\tau \cdot e^{j\theta_{\text{shift}}}} & 1 \end{bmatrix}. \tag{4}$$

According to [21], it is assumed that all voltage magnitudes are near to idea value 1 pu, and voltage angles are small and can assume $\cos(x) \approx 1$ and. $\sin(x) \approx x$. Thus, the power flow is expressed by

$$P_f = \text{Re}\left\{V_f \cdot I_f^*\right\} = \frac{\theta_f - \theta_t - \theta_{\text{shift}}}{X_s \cdot \tau}, \tag{5}$$

where θ_f and θ_t denote the voltage phase angle at the form and to end of a branch, and θ_{shift} is the phase angle of transformer ratio. On the other hand, the power flow at the end is $P_t = -p_f$ since the line is lossless. There, the nodal power injections are given by
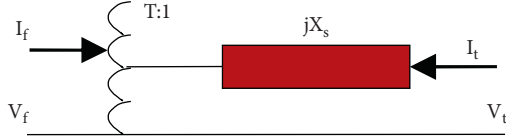
Figure 3: A branch model.

$$P_{\text{bus}} = B_{\text{bus}} \cdot \Theta + P_{\text{bus,shift}}, \tag{6}$$

where B_{bus} denotes the susceptance, Θ indicates the vector of bus voltage phase angles, and P_f can be given by

$$P_f = B_f \cdot \Theta + P_{f,\text{shift}}. \tag{7}$$

From circuit theory, the following relation can be written:

$$B_f = \text{diag}(B_{ff}) \cdot A^T, \tag{8}$$

$$B_{\text{bus}} = A \cdot B_f, \tag{9}$$

where B_{ff} shows an $N_L \times 1$ vector whose ith part is given by

$$B_{ff(i)} = \frac{1}{X_{s(i)} \cdot \tau_i}. \tag{10}$$

The dimension of occurrence matrix A is $N_B \times N_L$, and it presents the information of connected branches and nodes. (j, i) th and (k, i) th parts of matrix 1 and -1, if line i connected two buses j and k and other parts of A will be zero. Vector $P_{f,\text{shift}}$ indicates a dimension $N_L \times 1$, and its ith element is $-\theta_{\text{shift}} \cdot B_{ff(i)}$, $-\theta_{\text{shift}} \cdot B_{ff(i)}$; one gets

$$P_{\text{bus,shift}} = A \cdot P_{f,\text{shift}}. \tag{11}$$

Vector is

$$P_{\text{bus}} = P_g - P_d, \tag{12}$$

where P_g and P_d indicate vectors containing generator and demand powers, respectively. Matrix B_{bus} indicates the same as B' in the fast-decoupled power flow, and it gives up sensitivities of lines. It is filled in an $N_L \times N_B$ matrix and known as PTDF which is typically indicated by H and can be formulated by $N_L \times (N_B - 1)$ matrix [30]:

$$\widehat{H}_k = \widehat{B}_f \cdot B_{dc}^{-1}, \tag{13}$$

where $N_G, N_L,$ and N_B are the number of branches, busbars, and generators. $\widehat{B}_f$ is calculated by B_f and B_{bus} with reducing the reference bus. B_{dc} is calculated by taking out row k from B_{bus}. H is calculated by $\widehat{H}_k$ by putting in a column of zeros at column k. Bus 1 is usually considered the slack bus. In total, the relation between lines and buses is given by

$$P_b = H \cdot P_{inj}, \tag{14}$$

where P_b includes the line power flows, whereas P_{inj} includes the bus power injections.

2.3. Reduction of PTDF Matrix.
Reduction of the PTDF matrix is done in two steps of column reduction and row reduction.

2.3.1. Column Reduction.
If we replace the H-columns by placing the generator bus columns and the other load bus columns, Eq. (14) can be rewritten as follows:

$$P_b = [\, H_1 \quad H_2 \,] \cdot \begin{bmatrix} P_{gg} \\ -P_{dd} \end{bmatrix} = H_1 \cdot P_{gg} - H_2 \cdot P_{dd}, \tag{15}$$

where H_1 and H_2 indicate submatrices H, respectively, which have columns for generator and load nodes, and P_{gg} and P_{dd} indicate vectors with the power of generator and load nodes, respectively. If there are several generators in a single bus, in H_1 the corresponding bus column of H must be included several times. On the other hand, it is possible to replace multiple connected generators with a single bus with a single generator by means of the suitable cost function and power constraints. Also, if there is both output and load in a bus, the corresponding bus column of H must be included in both H_i $(i = 1, 2)$. The relationship between branch current and generator power output can be established in the following way:

$$P_b = H_g \cdot P_{gg}. \tag{16}$$

Combining (15) and (16), we obtain

$$H_g \cdot P_{gg} = H_1 \cdot P_{gg} - H_2 \cdot P_{dd}. \tag{17}$$

This can be used to calculate columns of H_g.

2.3.2. Row Reduction.
In DCOPF formulation, each unit is limited by its operation boundaries:

$$-P_b^{\text{max}} \leq P_b \leq P_b^{\text{max}}, \tag{18}$$

$$P_{gg}^{\text{min}} \leq P_{gg} \leq P_{gg}^{\text{max}}, \tag{19}$$

where P_b^{max} denotes the vector by means of branch MW ratings, and P_{gg}^{min} and P_{gg}^{max} indicate the minimum and maximum generator outputs (MW), respectively. For some branches, restrictions (18) may be nonbinding, showing that they can be removed and decrease the number of restrictions. Branch removal in the DC model is based on (16) by removing rows from the H_g matrix and the power flow i[th] branch is given as follows:

$$P_{b(i)} = H_g^{\langle \text{row}i \rangle} \cdot P_{gg}, \tag{20}$$

where the character $\langle \text{row}i \rangle$ shows i[th] row. Equation (20) is used twice for each branch to confirm whether their power limit is not binding. If the power boundary of line i is unconnected, the corresponding row of the Hg matrix will be removed.

2.4. Dynamic DCOPF.
Equations (21)–(29) show the DDCOPF problem formulations. Equation (21) is the

objective function of the proposed problem and other relations are the constraints of the OPF [24]:

$$\min \sum_{t=1}^{T} \left\{ \sum_{g=1}^{N_g} a_g + b_g P_{g,t} + c_g P_{g,t}^2 \right\}, \qquad (21)$$

subject to

$$P_g^{\min} \le P_{g,t} \le P_g^{\max}, \quad g = 1, 2, \ldots, N_g, \qquad (22)$$

$$\theta_i^{\text{ref}} \le \theta_{i,t} \le \theta_i^{\text{ref}}, \quad i \in I_{\text{ref}}, \qquad (23)$$

$$B_{\text{bus}}\theta_t + P_{\text{shift,bus},t} + P_{D,t} + G_{\text{shunt}} - E_{\text{gen}}P_{\text{gen},t} = 0, \qquad (24)$$

$$P_{\text{shift,bus},t} = (Z_{\text{from}} - Z_{\text{to}})^{\text{Trn}} P_{\text{shift,line},t}, \qquad (25)$$

$$P_{\text{shift,line},t} = P_{\text{line},t} - B_{\text{line}}\theta_t, \qquad (26)$$

$$B_{\text{line}} = B_{\text{line-line}}(Z_{\text{from}} - Z_{\text{to}}), \qquad (27)$$

$$B_{\text{line}}\theta_t + P_{\text{shift,line},t} - \text{MAX}_{\text{line}} \le 0, \qquad (28)$$

$$-B_{\text{line}}\theta_t - P_{\text{shift,line},t} - \text{MAX}_{\text{line}} \le 0, \qquad (29)$$

where $a_g, b_g,$ and c_g are the generator cost's coefficients, $P_{g,t}$ is the generated power of the gth generator at the ith hour, $P_g^{\min}$ and $P_g^{\max}$ are the minimum and maximum boundaries of the gth unit, $\theta_{i,t}$ is the bus voltage angle at the t$^{\text{th}}$ hour, θ_i^{ref} is the reference angle, G_{shunt} indicates the quantity of required power by means of the shunt components, and E_{gen} indicates the matrix of active units at each bus. Z_{from} and Z_{to} denote the matrices (a, b). Components of Z_{from} and Z_{to} for the connected line from bus b to c are 1, else, zero. $B_{\text{line-line}}$ is an $N_{\text{line}} \times 1$ matrix where its i$^{\text{th}}$ component is equal to $1/\tau^i \times x_s^i$.

2.5. Economic Formulation of Flexible Load.

Since the consumers have a changeable pattern during a day or period, it is necessary to consider the cross-time elasticity. It is defined with cross-time coefficients and relates the effect of price varying at one point in time to usage at other time periods. Hereby, the sensitivity of load to price is defined as elasticity and can be formulated by [2]

$$\text{Els}(t, t') = \frac{\rho_0(t')}{d_0(t)} \frac{\partial d(t)}{\partial \rho(t')} \begin{cases} \text{Els}(t, t') \le 0, & \text{if } t = t', \\ \text{Els}(t, t') \ge 0, & \text{if } t \ne t', \end{cases} \qquad (30)$$

where $d(t)$ denotes the load demand after implementing DR, $d_0(t)$ denotes the initial value of the load, $\text{Els}(t, t')$ denotes the elasticity in the price elasticity matrix, and $\rho_0(t')$ and $\rho(t')$ are the initial and current the electricity price after implementing DR, respectively. The elasticity coefficient $\text{Els}(t, t')$, with a negative rate, shows the elasticity intended for load varying at time t related to price varying. In the same way, a positive rate shows the elasticity for load change at time t caused by price change at time period t'. Self- and

cross-elasticity contents are presented as a 24×24 price elasticity matrix (PEM) by the following equation during a day:

$$\begin{bmatrix} \dfrac{\Delta d(1)}{d_0(1)} \\[6pt] \dfrac{\Delta d(2)}{d_0(2)} \\[6pt] \dfrac{\Delta d(3)}{d_0(3)} \\[6pt] \cdots \\[6pt] \dfrac{\Delta d(24)}{d_0(24)} \end{bmatrix} = \begin{bmatrix} \text{Els}(1,1) & \cdots & \text{Els}(1,24) \\ \vdots & \ddots & \vdots \\ \text{Els}(24,1) & \cdots & \text{Els}(24,24) \end{bmatrix} \times \begin{bmatrix} \dfrac{\Delta \rho(1)}{\rho_0(1)} \\[6pt] \dfrac{\Delta \rho(2)}{\rho_0(2)} \\[6pt] \dfrac{\Delta \rho(3)}{\rho_0(3)} \\[6pt] \cdots \\[6pt] \dfrac{\Delta \rho(24)}{\rho_0(24)} \end{bmatrix}. \qquad (31)$$

It is noted that with the linearity supposition, the above matrix relates the demand response model for NT time periods. The jth column of this matrix shows the price variations in the jth hour on the load profile. Also, the requested net profit is formulated by

$$NP(t) = \text{Ben}(d(t)) - d(t)\rho(t), \qquad (32)$$

where $\text{Ben}(d(t))$ indicates the obtained benefit by customers. In addition, the net profit, i.e., $NP(t)$ is computed by subtracting the price of electricity, i.e., $d(t)\rho(t)$ from profit from electricity sale:

$$\frac{\partial N\,P(t)}{\partial d(t)} = \frac{\partial \text{Ben}(d(t))}{\partial d(t)} - \rho(t) = 0, \qquad (33)$$

$$\frac{\partial \text{Ben}(d(t))}{\partial d(t)} = \rho(t). \qquad (34)$$

Taylor's series of Ben is as [24]

$$\text{Ben}(d(t)) = \text{Ben}(d_0(t)) + \frac{\partial \text{Ben}(d_0(t))}{\partial d(t)}[d(t) - d_0(t)]$$
$$+ \frac{1}{2} \frac{\partial^2 \text{Ben}(d_0(t))}{\partial d^2(t)}[d(t) - d_0(t)]^2, \qquad (35)$$

$$\text{Ben}(d(t)) = \text{Ben}(d_0(t)) + \rho_0(t)[d(t) - d_0(t)]$$
$$+ \frac{1}{2} \frac{\rho_0(t)}{\text{Els}(t,t)d_0(t)}[d(t) - d_0(t)]^2. \qquad (36)$$

The necessary state to appreciate the mentioned objective is to have

$$\frac{\partial \text{Ben}(d(t))}{\partial d(t)} = \rho_0(t)\left(1 + \frac{d(t) - d_0(t)}{\text{Els}(t,t)d_0(t)}\right). \qquad (37)$$

By combining Equations (37) and (34), for the single-period form of the responsive load,

$$d(t) = d_0(t) \times \left(1 + \frac{\rho(t) - \rho_0(t)}{\rho_0(t)} Els(t,t) \right). \qquad (38)$$

The multiperiod structure is given by

$$d(t) = d_0(t) \times \left\{ 1 + \sum_{\substack{t'=1 \\ t' \neq t}}^{24} Els(t,t') \times \frac{\rho(t') - \rho_0(t')}{\rho_0(t')} \right\}. \qquad (39)$$

It is practical to suppose that consumers will constantly want a level of demand d_i to make the most of their total benefits which are the difference in incomes from consuming electricity and incurred costs. Lastly, the finalized model is expressed as follows:

$$d(t) = d_0(t) \times \left\{ 1 + \sum_{t'=1}^{24} Els(t,t') \times \frac{\rho(t') - \rho_0(t')}{\rho_0(t')} \right\}. \qquad (40)$$

Based on Equation (40), $d(t)$ is related to $d_0(t)$, $Els(t,t')$, $\rho_0(t')$, and $\rho(t')$. If DRP is not implemented, there is no demand change ($d(t) = d_0(t)$).

Some features are introduced in the following equations to demonstrate the effects of applying DRPs on the demand profile [24]:

(i) The smoothness factor is preferably 100% which illustrates that load is constant and does not change with time:

$$LF\% = 100 \times \left(\frac{\sum_{t=1}^{T} d(t)}{T \times d^{\max}(t)} \right), \qquad (41)$$

where $d^{\max}(t)$ is the maximum load demand.

(ii) Peak to valley illustrates the distance ratio among peaks to the valley:

$$PTV\% = 100 \times \left(\frac{d^{\max}(t) - d^{\min}(t)}{d^{\max}(t)} \right). \qquad (42)$$

(iii) Peak compensation illustrates the normalized amount of compensated peak after implementing DRPs:

$$PC\% = 100 \times \left(\frac{d_0^{\max}(t) - d^{\max}(t)}{d_0^{\max}(t)} \right). \qquad (43)$$

The above equation denotes that after the achievement of DRPs the amount of peak decreases; this factor, i.e., peak recompense, essentially expresses the normalized quantity of this reduction.

2.6. Probabilistic Model of Wind Turbine Power Generation. The distributed generation resource used in this paper is based on wind technology. The constant power factor model

(constant active/reactive power) is used for this purpose [31]. In other words, this model is used for controllable distribution generations such as wind turbines with an independent controller of active and reactive power and synchronous generators with an excitation voltage regulator and power factor controller. In this model, the DG bus can be considered a PQ bus. The output of wind sources is a random variable due to random changes in wind speed. Depending on the wind speed, the output power of the wind turbine varies, so that at speeds between cut-in speed (V_{ci}) and rated speed (V_r), the output power is a linear function of wind speed and rated wind turbine power (P_r). At higher speeds up to cut-out speeds (V_{co}), the turbine output power remains constant at the rated value. At speeds above V_{co}, as well as at speeds below V_{ci} due to mechanical and safety issues, the turbine output power will be zero. According to these cases, the wind turbine power generation is calculated by

$$P(v) = \begin{cases} \dfrac{P_r}{V_r - V_{ci}} \times (v - V_{ci}), & V_{ci} \leq v \leq V, \\ \\ P_r, & V_r \leq v \leq V_{co}, \\ \\ 0, & \text{otherwise.} \end{cases} \qquad (44)$$

It can also be shown as the wind turbine's active power curve versus wind speed. For example, this curve for a V47-660 kW wind turbine generator is shown in Figure 4. The cut-in, rated, and cut-out speed values are 4, 15, and 25 (m/s), respectively. In this curve, the amount of wind generator output power is shown for each wind speed.

The sampling method can be used to determine the probability density function (PDF) of wind turbine power. In this technique, after determining the PDF wind speed and by sampling this probability distribution function, the output power of the turbine is determined using Equation (44) or the wind power curve, for each sample. The histogram curve is then plotted for all of the obtained samples. By this curve and fitting methods, the best probability distribution function for Wind turbine generated power can be obtained.

2.7. Proposed Framework. Figure 5 shows how to determine the optimal paths for DR implementation as a flowchart. Initially, the primary input data is defined; it can consist of load profile, electricity price, price-based program, and wind power. Subsequently, the PTDFs are computed and the DDCOPF can be solved for all hours, and the ATC index values are measured consequently. To calculate the power flow at all times, the counter is adjusted with parameter t. After that, the optimal buses for the installation of DGs are determined. For this purpose, PTDFs and the amount of loads on the system must be considered at the same time. It is worth that in all hours, the critical branches considering their ATC quantities are selected, and according to their PTDFs and power flow, the best buses for the most favorable execution of TOU-CPP are chosen. It can be seen from this
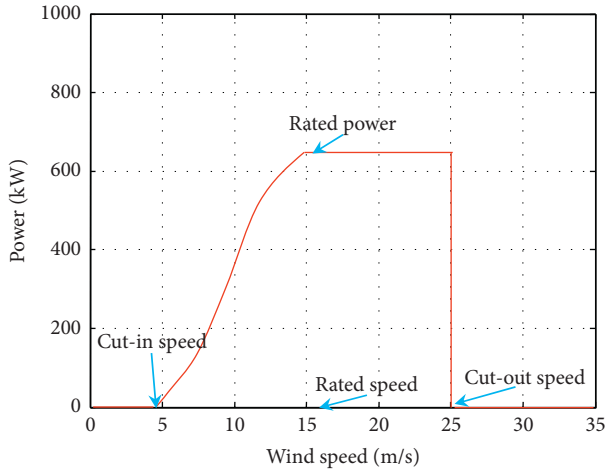
Figure 4: 660 kW wind farm turbine power curve.

figure that the solution procedure tries at creating the ATC positive for all branches during the day. Nevertheless, it may probable that after solving the proposed problem for all hours, ATC returns negative values for several branches in accordance with the power network structure. For instance, if PTDFs indicate the positive values for a number of lines at various hours, this technique can not reduce the congestion. In this condition, the following options are considered: (i) rising the number of selected nodes for executing the DRPs, (ii) employing DG at the critical nodes as negative loads, (iii) diminishing generated power at the critical nodes, and (iv) making the new or critical branches. Note that the main aim of this process is finding the optimal bus to install the distributed generation. The optimal bus is found after the proposed power flow considered the demand response program which shows the power demand flexibility to make a flat shape of the profile. The final result is better performance of the power system without congestion and an acceptable voltage profile.

3. Simulation Result

To evaluate the correctness and applicability of the proposed method, it is applied to the IEEE 39-bus New England test system (see Figure 6). There are 29 load buses in the 39 bus test system. Information about system lines is given in Table 1, and the other network information is given in [32]. According to Table 2, the base load information is considered according to the 39 bus system information, and the load information within 24 hours is assumed to be in the ratio mentioned in [32]. In order to match the hourly and base load, the base load of the system has been reduced by 2.5 times. It is necessary to say that the amount of demand for all buses is enlarged by 5% and to make the load dynamic for 24 hours. The electricity prices in the valley, off-peak, and peak periods are low, average, and high, respectively. Here, the average electricity price is 15 $/MWh in the off-peak, 12 $/MWh in the valley, and 20 $/MWh in the peak period. Therefore, buses 1, 3, 4, 18, and 26 are determined as critical ones. According to Table 3, the daily load curve is divided
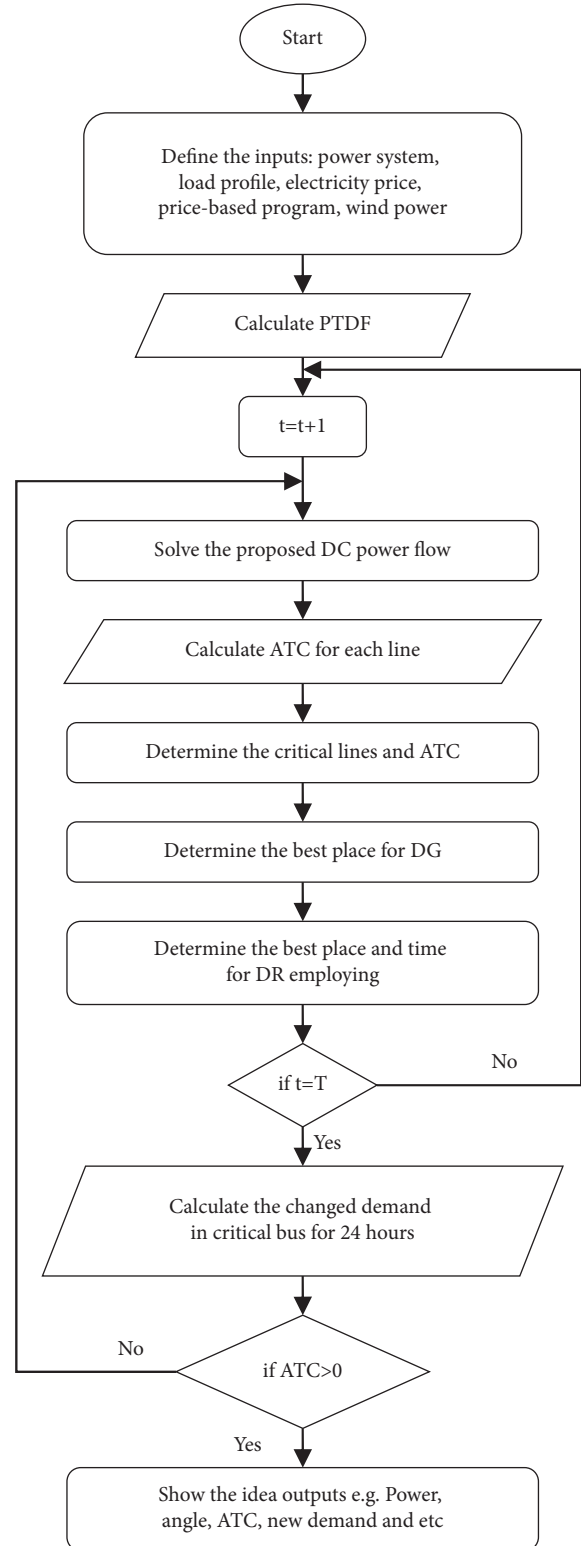

Figure 5: Solution method's flowchart.

into the peak (19–24 hours), off-peak (9–18 hours), and valley (1–8 hours) periods. The hour 21 : 00 is selected as the critical peak hour, and the CPP is implemented at this time. Based on this table, the electricity cost has its highest and lowest values for critical peak and valley hours, respectively.
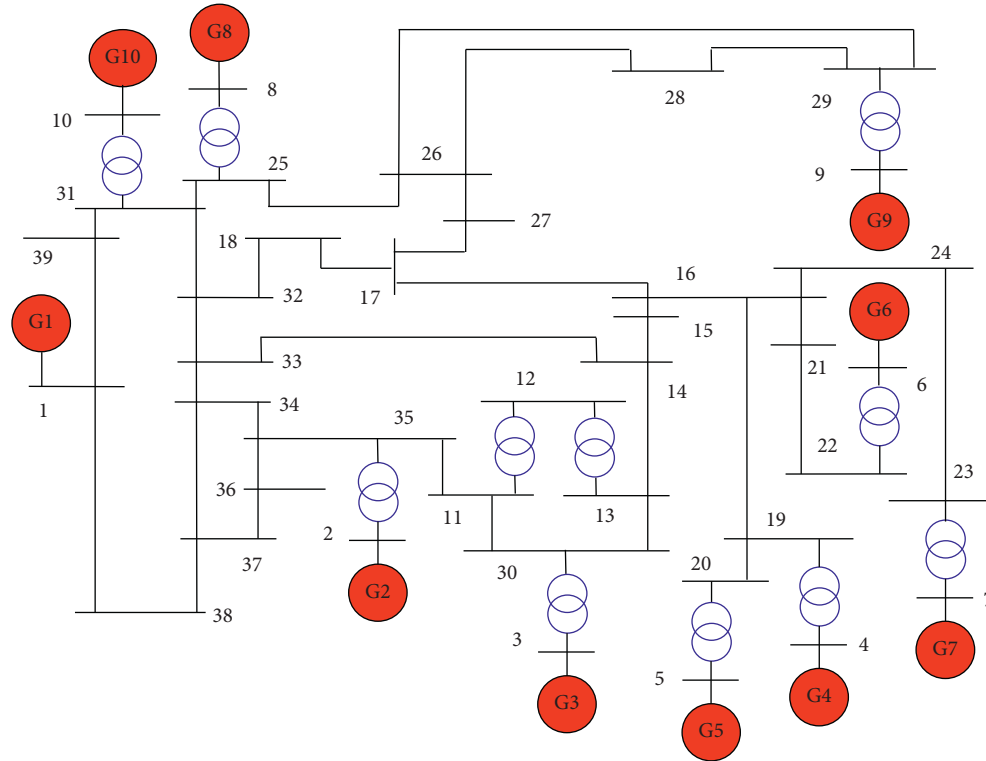
FIGURE 6: 10-machine 39-buses system structure case study.

TABLE 1: Test system lines information.

From	To	R (pu)	X (pu)	Bc (pu)	From	To	R (pu)	X (pu)	Bc (pu)
1	2	0.0035	0.0411	0.6987	14	15	0.0018	0.0217	0.366
1	39	0.001	0.025	0.75	15	16	0.0009	0.0094	0.171
2	3	0.0013	0.0151	0.2572	16	17	0.0007	0.0089	0.1342
2	25	0.007	0.0086	0.146	16	19	0.0016	0.0195	0.304
2	30	0	0.0181	0	16	21	0.0008	0.0135	0.2548
3	4	0.0013	0.0213	0.2214	16	24	0.0003	0.0059	0.068
3	18	0.0011	0.0133	0.2138	17	18	0.0007	0.0082	0.1319
4	5	0.0008	0.0128	0.1342	17	27	0.0013	0.0173	0.3216
4	14	0.0008	0.0129	0.1382	19	20	0.0007	0.0138	0
5	6	0.0002	0.0026	0.0434	19	33	0.0007	0.0142	0
5	8	0.0008	0.0112	0.1476	20	34	0.0009	0.018	0
6	7	0.0006	0.0092	0.113	21	22	0.0008	0.014	0.2565
6	11	0.0007	0.0082	0.1389	22	23	0.0006	0.0096	0.1846
6	31	0	0.025	0	22	35	0	0.0143	0
7	8	0.0004	0.0046	0.078	23	24	0.0022	0.035	0.361
8	9	0.0023	0.0363	0.3804	23	36	0.0005	0.0272	0
9	39	0.001	0.025	1.2	25	26	0.0032	0.0323	0.531
10	11	0.0004	0.0043	0.0729	25	37	0.0006	0.0232	0
10	13	0.0004	0.0043	0.0729	26	27	0.0014	0.0147	0.2396
10	32	0	0.02	0	26	28	0.0043	0.0474	0.7802
12	11	0.0016	0.0435	0	26	29	0.0057	0.0625	1.029
12	13	0.0016	0.0435	0	28	29	0.0014	0.0151	0.249
13	14	0.0009	0.0101	0.1723	29	38	0.0008	0.0156	0

3.1. Results of DR and DG Installation Programs. In this paper, the optimal placement of DG and the DRPs is exploited concurrently to improve the network loading capability, reduce power peaks, and increase the ATC of transmission lines. The concurrent utilization of these methods guarantees that the operational point is optimum

and the generation and imposed costs for customers are at the minimum values. In order to select the optimal buses with the most negative amount of PTDF, buses 3 and 4 are selected due to their higher load and significance of load shedding for the installation of distributed wind generations. It is considered that there is a wind farm with a total rated

TABLE 2: Test system load information.

Bus	Pd (MW)	Qd (MVAR)	Bus	Pd (MW)	Qd (MVAR)	Bus	Pd (MW)	Qd (MVAR)
1	97.6	44.2	14	0	0	27	281	75.5
2	0	0	15	320	153	28	206	27.6
3	322	2.4	16	329	32.3	29	283.5	26.9
4	500	184	17	0	0	30	0	0
5	0	0	18	158	30	31	9.2	4.6
6	0	0	19	0	0	32	0	0
7	233.8	84	20	680	103	33	0	0
8	522	176.6	21	274	115	34	0	0
9	6.5	−66.6	22	0	0	35	0	0
10	0	0	23	247.5	84.6	36	0	0
11	0	0	24	308.6	−92.2	37	0	0
12	8.53	88	25	224	47.2	38	0	0
13	0	0	26	139	17	39	1104	250

capacity of 50 MW in each of these two buses. The statistical information of wind in a specific area is considered for obtaining the probability model of wind turbines. The mentioned model of the wind farm is attained through the sampling of the wind speed. According to [31], the best probability distribution for wind speed modeling is the Weibull probability distribution. Therefore, the density function of wind speed in the mentioned area is a Weibull distribution with c and k variables equal to 7.43 and 2.49, which is related to the standard variations of wind speed. It is considered that the cut-in and cut-out speeds and the rated speed of wind power plants in this area are 2, 25, and 10 m/s, respectively, which are in the standard range of the real turbines. Consider that the generated power of the mentioned turbine at different wind speeds is known; thus, at a specific wind speed, the turbine output is obtained by employing the power-wind curve. Therefore, the histogram of the wind-generated power is obtained through 10000 runs of the simulation, as shown in Figure 7. According to the simulation program, this number of simulation runs leads to the convergence of results. In other words, the generated power of each wind farm in the installed buses can be calculated by the probability distribution function, which is fitted on the histogram. In these figures, the vertical axis demonstrates the number of each occurred sample.

Generally, the DRPs are implemented on critical buses. The power transmission and distribution coefficients are calculated at critical hours to detect the critical buses. Buses with the most negative coefficients are the most suitable and effective ones in the problem. Since these buses have the highest impression on reducing the congestion, employing the DRPs on these buses results in alleviating the congestion and an increase in the ATC of critical lines; the numerical results are shown in Figure 8.

According to this curve, concurrent implementation of the DRPs and installation of wind generators shift the system load from peak hours to the valley and average load hours; thus, the overall load of the system is decreased, especially in critical hours. It is clear that implementing the DGs in addition to demand response management programs supplies the system load locally and reduces the distance between peak to valley and energy generated by thermal power stations. They also reduce the loss and improve load
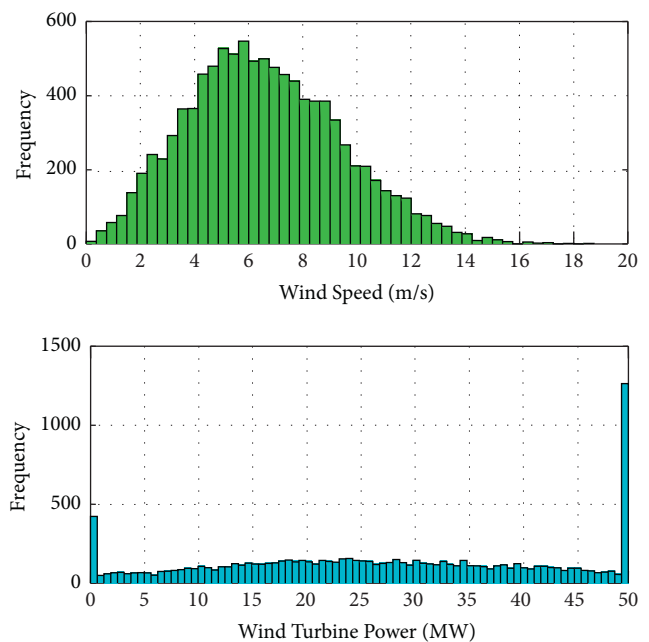

FIGURE 7: Wind speed histogram in the mentioned area and wind-generated power histogram.

coefficient and optimal generation planning. At the same time, Figure 9 demonstrates that the installation of DGs, with a focus on the loss and cost reduction issues, reduces the total imposed costs of the system. The utilization of the DRPs without the installation of DGs does not lead to a significant reduction in costs.

The ATC values for the critical hours (i.e., 20:00 to 22:00) before and after the implementation of the DRPs and DG installation are given in Figures 10–12. According to Figure 10, there are ten critical lines in the system at 20:00. ATCs for most of the lines are increased after concurrent utilization of DRPs and installation of wind farms at buses 3 and 4. This increase is higher than the case in which only the TOU-CPP has been implemented, especially in lines 6, 7, 14, and 18. On the other hand, at 21:00, which is the most critical hour of the system, the ATC is near zero at 12 lines of the system. However, after concurrent implementation of TOU-CPP at 21:00 and installation of wind generations, the
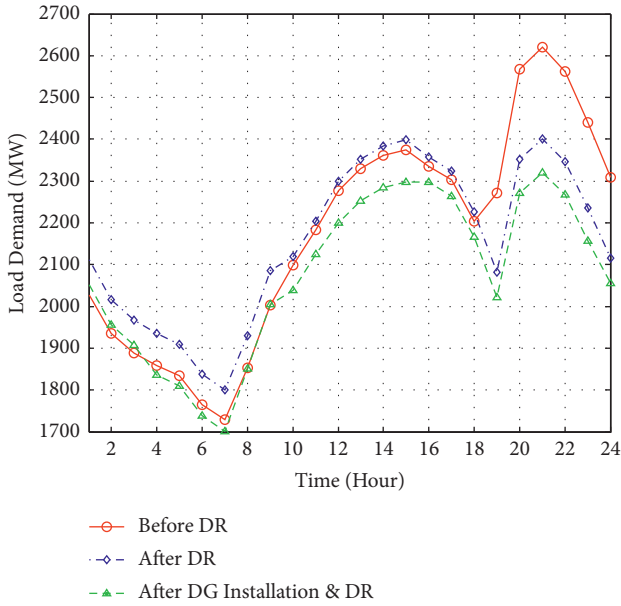
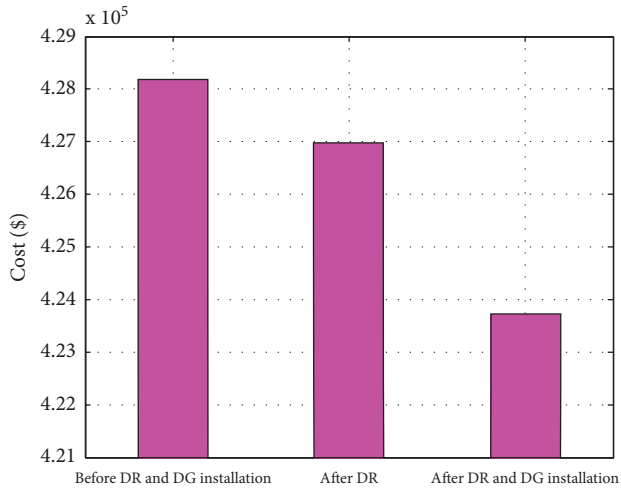FIGURE 8: The total load of the system 24 hours before and after implementation of DRPs and installation of DGs.

FIGURE 9: Comparison of total exploitation costs before and after installation of DGs and implementation of DRPs.

FIGURE 10: ATC values of critical lines at 20 : 00, before and after implementing the DRPs and DG installation.
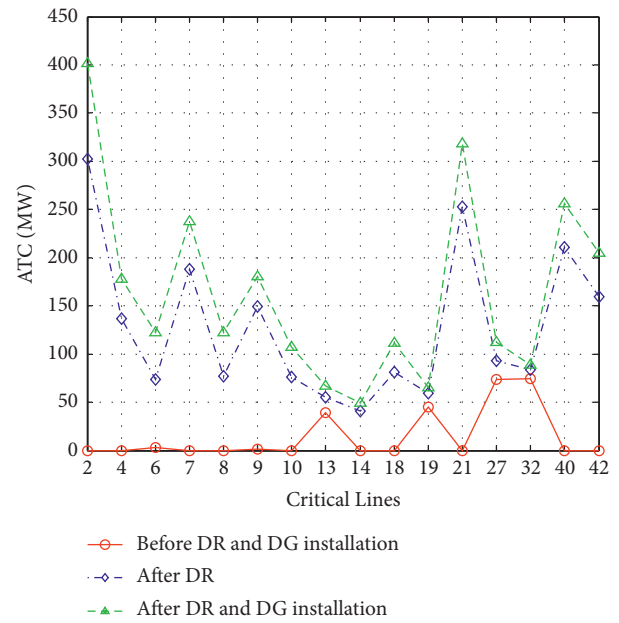
FIGURE 11: ATC values of critical lines at 21 : 00, before and after implementing the DRPs and DG installation.

minimum ATC is increased from zero to 49.3 MW corresponding to line 14. Also, the ATC value in line 2 had an increase of about 100 MW. At 22 : 00, line 14 has the minimum ATC, which is increased from 7 MW to 100 MW after implementing the TOU-CPP and DG installation. In this situation, the ATC is increased significantly in lines 2, 6, 7, 8, and 10.

A comparison is made to evaluate the effect of the proposed method on the technical parameters of the network. Accordingly, Table 4 demonstrates the voltages of load buses in the network before and after implementing the DRPs and placement of DGs. As shown in the table, the highest increase in voltage has occurred at buses 3 and 4 (about 7%), since the DGs are installed on these buses. Also, the nearby buses have experienced a significant increase in
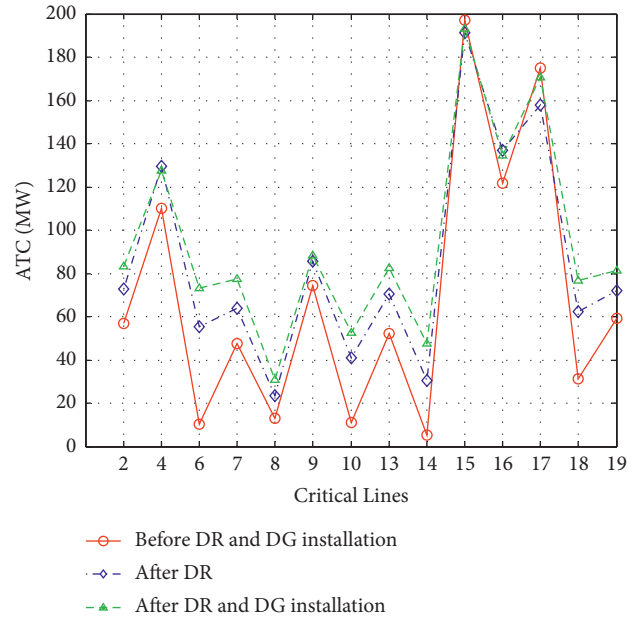
voltage. Although the DRPs are efficient for the improvement of the bus voltages, especially in critical loadings and peak hours, the voltage increase mainly depends on the installation of distributed wind generations. In this situation, the lowest network voltage in bus no. 20 is increased from 0.94 to 0.96 at peak hour. Therefore, even in the worst case, the voltage drop of the network will not be more than 4%. On the other hand, based on the proper choice of parameters for the distributed generation capacity, the overvoltage in the nearby buses remains in the standard range and does not exceed more than 5%.
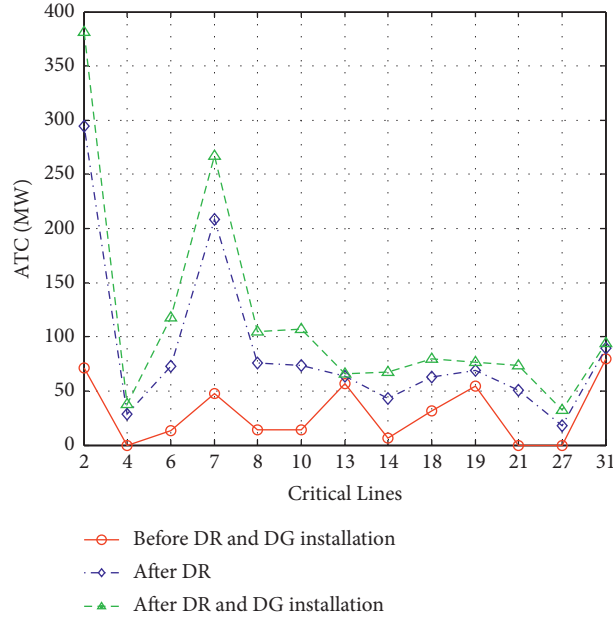
FIGURE 12: ATC values of critical lines at 22 : 00, before and after implementing the DRPs and DG installation.

TABLE 3: Information of DRPs.

DR program	CPP		TOU	
Actived time	21	19–24	9–18	1–8
Price ($/MWh)	50	20	15	12

TABLE 4: Voltages of load buses in the network before and after concurrent implementation of DRPs and DG installation.

Bus	Voltage (pu)		Bus	Voltage (pu)	
	Before program	After program		Before program	After program
1	0.99	1.02	16	0.98	1.00
2	1.00	1.05	17	0.97	1.01
3	0.98	1.05	18	0.97	1.02
4	0.96	1.03	19	1.00	1.01
5	0.96	1.01	20	0.94	0.96
6	0.96	1.00	21	0.98	0.99
7	0.95	0.99	22	0.99	1.00
8	0.95	0.99	23	0.99	1.00
9	0.97	0.99	24	0.99	1.01
10	0.97	0.99	25	1.01	1.04
11	0.97	0.99	26	1.00	1.02
12	0.95	0.97	27	0.97	0.99
13	0.95	1.00	27	1.00	1.01
14	0.96	1.01	28	1.00	1.01
15	0.96	0.99			

TABLE 5: Total costs and system loss before and after implementation of the proposed method.

Parameter	After program	Before program
Total cost ($)	423723	428195
Loss in peak (MW)	21.74	24.18

Table 5 exhibits the total generation costs in the system before and after the implementation of the proposed program. According to this table, the total costs after implementation of the programs are reduced by 4472 $. This fact demonstrates that implementing a suitable method to alleviate the system congestion not only improves the ATC but also reduces the system costs to a reasonable amount. On the other hand, this table shows that the implementation of these programs reduces the system loss from 24.18 MW to 21.74 MW, which is a 9% reduction. This result has various reasons. First, the decrease of load peak in critical hours can

be an effective reason for loss reduction, which is realized by the implementation of CPP and TOU programs. Furthermore, the optimal utilization of DGs' capability is a determinative factor in loss reduction. Although the critical lines of the system determine the installation place of these generations, their installation generally reduces the total loss of the system since the nearby generation centers feed these load centers, which reduces the current flows in lines and consequently reduces their loss.

4. Conclusion

In this paper, a new procedure for CM was presented. The proposed method implemented two approaches concurrently: the demand side management methods and the installation of DGs at the critical buses of the system. Both approaches determine the critical buses of the system for participating in DRPs and the installation of DGs by the implementation of PTDFs. Therefore, in addition to the reduction of exploitation costs, both methods participate the best and most effective buses for improving the system ATC. In order to solve the optimization problem, it has been modeled as optimized and dynamic load distribution. The proposed method is applied to the IEEE 39-bus system. The results demonstrate the high performance and practical advantages of the proposed method. For instance, the available transmission capacity is zero for line 12 at 21:00, which is the most critical hour of the system. After concurrent utilization of load responding plans of CPP and TOU at 21:00 and installation of wind generations, the minimum ATC is increased from zero to 49.3 MW. Furthermore, the load curve analysis before and after method utilization confirms the improvements in curve parameters such as load coefficient and peak to valley interval. Moreover, a cost reduction of about 4500 $ is observed after utilization of the proposed method in 24 hours. The advantages and main results of the paper can be concluded as follows:

(i) The ATC of the system is improved, especially in critical buses and hours, the system performance in power transmission is enhanced, and transmission limitations in the network are omitted. In addition to power saving, it reduces the probability of unwanted power outages caused by overhead loads and increases system reliability. The method does not require more transmission infrastructures for energy transmission, and consequently, it reduces the costs.

(ii) The method decreases the total exploitation costs of the system and reduces electricity costs for subscribers. It also increases their satisfaction levels. Higher system reliability leads to shorter outage intervals and fewer electricity outages, which minimizes the imposed costs to the network and subscribers.

(iii) The method increases the contribution of renewable generation methods in load supply and lessens environmental pollution through a reduction in the

power generation of thermal plants. The addition of distributed generations to the system increases the generation capability of the network and provides an energy selling capability and more profits for the investors.

(iv) The network peak is decreased, and the indicators of peak to valley interval and load factor are enhanced. According to these results, the consumed power data in 24 hours will be closer to the average consumption value, and it resolves the requirements for excess plants to supply power in a few peak hours of the year. The loss of the network is reduced, and consequently, system performance is enhanced.

Data Availability

All data generated or analyzed during this study are included in this published article.

Conflicts of Interest

The authors declare that they have no conflicts of interest.

References

[1] X. Tai, H. Sun, and Q. Guo, "Electricity transactions and congestion management based on blockchain in energy internet," *Power System Technology*, vol. 40, no. 12, pp. 3630–3638, 2016.

[2] S. S. Kholerdi and A. Ghasemi-Marzbali, "Interactive Time-of-use demand response for industrial electricity customers: a case study," *Utilities Policy*, vol. 70, Article ID 101192, 2021.

[3] W. Huang, N. Zhang, C. Kang, M. Li, and M. Huo, "From demand response to integrated demand response: review and prospect of research and application," *Protection and Control of Modern Power Systems*, vol. 4, no. 1, pp. 1–13, 2019.

[4] B. Wang, X. Fang, X. Zhao, and H. Chen, "Bi-level optimization for available transfer capability evaluation in deregulated electricity market," *Energies*, vol. 8, no. 12, pp. 13344–13360, 2015.

[5] P. Kalaimani and K. M. Sundaram, "Congestion management with improved real power transfer using TCSC in 30 bus system," *International Journal of Information Technology and Management*, vol. 20, no. 1-2, pp. 66–82, 2021.

[6] E. Shayesteh, M. P. Moghaddam, S. Taherynejhad, and M. K. Sheikh-el-Eslami, "Congestion management using demand response programs in power market," in *Proceedings of the 2008 IEEE Power and Energy Society General Meeting-Conversion and Delivery of Electrical Energy in the 21st Century*, Pittsburgh, PA, USA, 2008.

[7] H. K. Nunna and S. Doolla, "Energy management in microgrids using demand response and distributed storage—a multiagent approach," *IEEE Transactions on Power Delivery*, vol. 28, no. 2, pp. 939–947, 2013.

[8] E. Shayesteh, A. Yousefi, M. P. Moghaddam, and G. R. Yousefi, "An economic comparison between incorporation of FACTS devices and demand response programs for ATC enhancement," in *Proceedings of the 2008 IEEE Canada Electric Power Conference*, Vancouver, BC, Canada, 2008.

[9] P. Samadi, H. Mohsenian-Rad, R. Schober, and V. W. Wong, "Advanced demand side management for the future smart

grid using mechanism design," *IEEE Transactions on Smart Grid*, vol. 3, no. 3, pp. 1170–1180, 2012.

[10] S. Ramchurn, P. Vytelingum, A. Rogers, and N. Jennings, "Agent-based control for decentralised demand side management in the smart grid," in *Proceedings of the 10th International Conference on Autonomous Agents and Multiagent Systems*, pp. 5–12, Prague, Czech Republic, May 2011.

[11] Z. Zhu, J. Tang, S. Lambotharan, W. H. Chin, and Z. Fan, "An integer linear programming based optimization for home demand-side management in smart grid," in *Proceedings of the 2012 IEEE PES Innovative Smart Grid Technologies (ISGT)*, Washington, DC, USA, 2012.

[12] A. Kumar and M. Kumar, "Available transfer capability determination using power transfer distribution factors," *International Journal of Information and Computation Technology*, vol. 3, no. 11, pp. 1035–1040, 2013.

[13] D. Šošić, I. Škokljev, and N. Pokimica, "Features of power transfer distribution coefficients in power system networks," *Infoteh-Jahorina*, vol. 13, pp. 86–90, 2014.

[14] M. Rahmani, A. Kargarian, and G. Hug, "Comprehensive power transfer distribution factor model for large-scale transmission expansion planning," *IET Generation, Transmission & Distribution*, vol. 10, no. 12, pp. 2981–2989, 2016.

[15] A. K. Barik and D. C. Das, "Coordinated regulation of voltage and load frequency in demand response supported bio-renewable cogeneration-based isolated hybrid microgrid with quasi-oppositional selfish herd optimisation," *International Transactions on Electrical Energy Systems*, vol. 30, no. 1, Article ID e12176, 2020.

[16] M. Muratori and G. Rizzoni, "Residential demand response: dynamic energy management and time-varying electricity pricing," *IEEE Transactions on Power Systems*, vol. 31, no. 2, pp. 1108–1117, 2015.

[17] F. Rahimi and A. Ipakchi, "Demand response as a market resource under the smart grid paradigm," *IEEE Transactions on Smart Grid*, vol. 1, no. 1, pp. 82–88, 2010.

[18] H. Abdi, E. Dehnavi, and F. Mohammadi, "Dynamic economic dispatch problem integrated with demand response (DEDDR) considering non-linear responsive load models," *IEEE Transactions on Smart Grid*, vol. 7, no. 6, pp. 2586–2595, 2015.

[19] E. Dehnavi and H. Abdi, "Optimal pricing in time of use demand response by integrating with dynamic economic dispatch problem," *Energy*, vol. 109, pp. 1086–1094, 2016.

[20] F. Zaeim-Kohan, H. Razmi, and H. Doagou-Mojarrad, "Multi-objective transmission congestion management considering demand response programs and generation rescheduling," *Applied Soft Computing*, vol. 70, pp. 169–181, 2018.

[21] A. Yousefi, T. T. Nguyen, H. Zareipour, and O. P. Malik, "Congestion management using demand response and FACTS devices," *International Journal of Electrical Power & Energy Systems*, vol. 37, no. 1, pp. 78–85, 2012.

[22] M. A. F. Ghazvini, G. Lipari, M. Pau et al., "Congestion management in active distribution networks through demand response implementation," *Sustainable Energy, Grids and Networks*, vol. 17, Article ID 100185, 2019.

[23] J. Wu, B. Zhang, Y. Jiang, P. Bie, and H. Li, "Chance-constrained stochastic congestion management of power systems considering uncertainty of wind power and demand side response," *International Journal of Electrical Power & Energy Systems*, vol. 107, pp. 703–714, 2019.

[24] E. Dehnavi and H. Abdi, "Determining optimal buses for implementing demand response as an effective congestion management method," *IEEE Transactions on Power Systems*, vol. 32, no. 2, pp. 1537–1544, 2016.

[25] S. Lv, Z. Wei, S. Chen, G. Sun, and D. Wang, "Integrated demand response for congestion alleviation in coupled power and transportation networks," *Applied Energy*, vol. 283, Article ID 116206, 2021.

[26] H. Ebrahimi, A. Yazdaninejadi, and S. Golshannavaz, "Demand response programs in power systems with energy storage system-coordinated wind energy sources: a security-constrained problem," *Journal of Cleaner Production*, vol. 335, Article ID 130342, 2022.

[27] M. Roustaei, A. Letafat, M. Sheikh, R. Sadoughi, and M. Ardeshiri, "A cost-effective voltage security constrained congestion management approach for transmission system operation improvement," *Electric Power Systems Research*, vol. 203, Article ID 107674, 2022.

[28] S. Voswinkel, J. Höckner, A. Khalid, and C. Weber, "Sharing congestion management costs among system operators using the Shapley value," *Applied Energy*, vol. 317, Article ID 119039, 2022.

[29] F. Shen, Q. Wu, X. Jin, M. Zhang, S. Teimourzadeh, and O. B. Tor, "Coordination of dynamic tariff and scheduled reprofiling product for day-ahead congestion management of distribution networks," *International Journal of Electrical Power & Energy Systems*, vol. 135, Article ID 107612, 2022.

[30] O. Ajayi, N. Nwulu, and U. Damisa, "Application of meta-heuristic algorithms in DC-optimal power flow," *African Journal of Science, Technology, Innovation and Development*, vol. 12, no. 7, pp. 867–872, 2020.

[31] M. Noshyar and A. Ghasemi-Marzbali, "Dynamic economic/emission dispatch with probability model of wind power with modified virus colony search algorithm," *Computational Intelligence in Electrical Engineering*, 2021.

[32] R. D. Zimmerman, C. E. Murillo-Sánchez, and D. Gan, *MATPOWER: A MATLAB power system simulation package*, Manual, Power Systems Engineering Research Center, Ithaca, NY, USA, 1997.